ELSEVIER

European Journal of Pharmacology 449 (2002) 207–211

ejp

www.elsevier.com/locate/ejphar

Size of side-chain at channel pore mouth affects Ca^{2+} block of $P2X_2$ receptor

Ken Nakazawa [a,b,*], Hideaki Sawa [a,c], Hiloe Ojima [a,c], Reiko Ishii-Nozawa [c], Koichi Takeuchi [c], Yasuo Ohno [b]

[a] *Cellular and Molecular Pharmacology Section, National Institute of Health Sciences, 1-18-1 Kamiyoga, Segataya, Tokyo 158-8501, Japan*
[b] *Division of Pharmacology, National Institute of Health Sciences, 1-18-1 Kamiyoga, Segataya, Tokyo 158-8501, Japan*
[c] *Department of Clinical Pharmacology, Meiji Pharmaceutical University, 2-522-1 Noshio, Kiyose, Tokyo 204-8588, Japan*

Received 7 March 2002; received in revised form 18 June 2002; accepted 25 June 2002

Abstract

Effects of amino acid replacement at the channel pore mouth of $P2X_2$ receptor/channel on multivalent cation channel block were investigated. When Asn^{333} was replaced with various amino acid residues with neutral side chains (Gly, Ala, Val, Leu and Ile), the block by Ca^{2+} was attenuated according to the sizes of the side chains. The block by La^{3+} was also greatest with the Gly-substituted mutant, but this preference was not found for the block by other multivalent cations tested. The side chain at the channel pore mouth may interfere with the access of Ca^{2+} block by steric hindrance.

Keywords: $P2X_2$ receptor; Ion channel; Ca^{2+}; Multivalent cation block; Site-directed mutagenesis; *Xenopus* oocyte

1. Introduction

P2X receptors are ion channel-forming proteins which are activated by extracellular ATP, and its roles in excitatory neurotransmission have been demonstrated in various tissues (Burnstock, 1997; Khah, 2001). To date, at least seven subclasses ($P2X_{1-7}$) have been cloned, and they have been shown to form homo- or heteromeric receptors which act as functional ion channels (North and Surprenant, 2000). The analysis of the hydropathy profiles of amino acid sequences of P2X receptors has shown that each subclass consists of two transmembrane domains (TM1 and TM2) and one long extracellular domain between them (E1). A line of experimental evidence supports the contribution of TM2 to the formation of the channel pore (Rassendren et al., 1997; Egan et al., 1998; Migita et al., 2001), and recent findings have also suggested the contribution of TM1 to the pore formation (Jiang et al., 2001; Haines et al., 2001). An asparagine residue at the position 333 in TM2 of $P2X_2$ receptor (Asn^{333}) is believed to exist near the outer mouth of the channel pore, and serve as a key residue which determines single-channel conductance (Nakazawa et al., 1998a). Asn^{333} appears to contribute to formation of the channel pore because the dilation of the channel pore upon long-lasting receptor activation was accelerated when this residue was replaced with alanine (Virginio et al., 1999). Ca^{2+} and other divalent cations (Nakazawa and Hess, 1993; Ding and Sachs, 1999, 2000; Negulyaev and Markwardt, 2000) and trivalent cations (Nakazawa et al., 1997) are known to inhibit ionic current permeating through P2X receptor/channels. In the present study, we replaced Asn^{333} of $P2X_2$ receptor/channel with various amino acids, and investigated the block by Ca^{2+} and other multivalent cations of these mutant channels to elucidate the interaction between these ions and the channel pore mouth.

2. Materials and methods

Mutants of $P2X_2$ receptor constructed from the cloned rat $P2X_2$ receptor (Brake et al., 1994) were kindly supplied by Prof. R.A. North, except for N333I, N333V, N333L and

* Corresponding author. Division of Pharmacology, National Institute of Health Sciences, 1-18-1 Kamiyoga, Segataya, Tokyo 158-8501, Japan. Tel.: +81-3-3700-9704; fax: +81-3-3707-6950.
E-mail address: nakazawa@nihs.go.jp (K. Nakazawa).

0014-2999/02/$ - see front matter © 2002 Elsevier Science B.V. All rights reserved.
PII: S0014-2999(02)02001-0

N333I, which were constructed by site-directed mutagenesis in our laboratory as described (Nakazawa et al., 1998b). Channels were expressed in *Xenopus* oocytes and ionic currents permeating through them were measured as previously described (Nakazawa and Ohno, 1996; Nakazawa et al., 1998b). Oocytes were bathed in ND96 solution containing (in mM) NaCl 96, KCl 2, $CaCl_2$ 1.8, $MgCl_2$ 1, HEPES 5 (pH 7.5 with NaOH). ATP (adenosine 5′ -triphosphate disodium salt; Sigma, St. Louis, MO, USA) was applied by superfusion for about 6 s with a regular interval of 1 min. All the divalent and trivalent cations used were chloride salts of reagent grade. The trivalents cations and Mn^{2+} were dissolved in standard ND96 solution. When block by Ca^{2+} or Mg^{2+} was assessed, these cations were dissolved in Ca^{2+}-free, Mg^{2+}-free ND96 solution. The current amplitude in the presence of trivalent cations and Mn^{2+} was normalized to that in the absence of these cations. Under divalent cation-free condition, *Xenopus* oocytes become electrically too leaky to record current responses to ATP because of the opening of divalent cation-sensitive nonselective cation channels (Arellano et al., 1995; Zhang et al., 1998). Thus, for the current block by Ca^{2+} or Mg^{2+}, the current amplitude was normalized to that in the presence of 0.18 mM Ca^{2+} or Mg^{2+}, respectively. Statistical analysis was first made by the analysis of variance (ANOVA) and, when *F*-values were statistically significant, the comparison of groups was made by Tukey's test. When statistical significance was stated, *F*- and *P*-values were listed in corresponding figure legends.

3. Results

By increasing extracellular Ca^{2+}, ionic current activated by 30 μM ATP was decreased (Fig. 1A). Fig. 1B compares

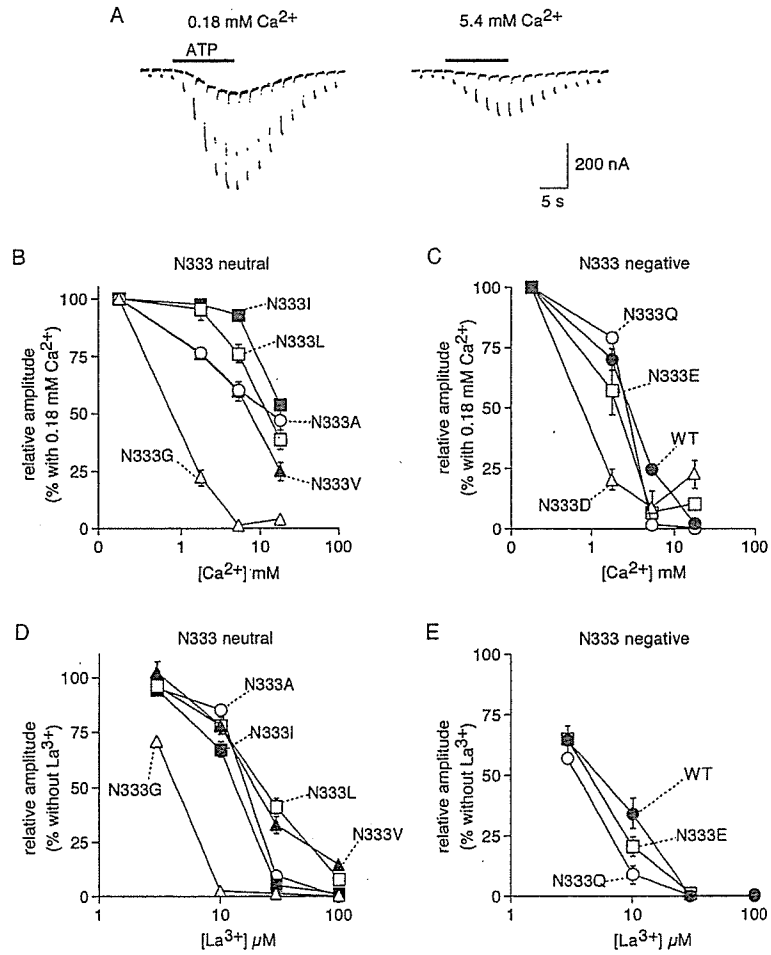

Fig. 1. (A) Ionic current activated by 30 μM ATP in a *Xenopus* oocyte expressing the wild type $P2X_2$ receptor/channel in the presence of 0.18 (left) or 5.4 mM Ca^{2+} (right). The oocyte was held at −50 mV and stepped for 400 ms to −80 mV every 2 s. (B–E) Concentration–response curve for Ca^{2+} (B, C) and La^{3+} (D, E) block on channels with neutral (B, D) or negatively polarized and charged (C, E) amino acid residues at the position 333. Current was measured as in (A), and responses at −80 mV were normalized to those in the presence of 0.18 mM Ca^{2+} or in the absence of the La^{3+} (see Section 2). The normalized responses are plotted against the logarithm of Ca^{2+} or La^{3+} concentrations. Each symbol and bar represent the mean and S.E. obtained from four to six oocytes tested. The values from the statistical analysis of the block by 5.4 mM Ca^{2+} are $F=135.6$ ($P<0.001$ by ANOVA) and $P<0.001$ (N333G vs. N333A), $P<0.01$ (N333A vs. N333L, N333V vs. N333I, N333L vs. N333I) or $P>0.05$ (N333A vs. N333V), and those of the block by 10 μM La^{3+} are $F=183.7$ ($P<0.001$ by ANOVA) and $P<0.001$ (N333G vs. N333A, N333G vs. N333V, N333G vs. N333G vs. N333L, N333G vs. N333I).

the block by Ca^{2+} of ionic current through $P2X_2$ receptor/channel mutants that possess amino acid residues with neutral side chains at position 333 (N333G, N333A, N333V, N333L and N333I). Among these neutral mutants, N333G was the most sensitive to Ca^{2+}, and the sensitivity was lowered almost completely according to the size of the side chains (Gly>Ala ≅ Val>Leu>Ile). This order was also statistically assured when the block by 5.4 mM Ca^{2+} was compared among these mutants. The block by La^{3+} was also greatest with N333G; the remaining neutral mutants uniformly exhibited lower sensitivities (Fig. 1D). The block by 10 μM La^{3+} was significantly greater with N333G than with the remaining four mutants.

Fig. 1C compares the block by Ca^{2+} of the channels that possess amino acid residues with negatively polarized (WT and N333Q) or charged (N333D and N333E) residues at the position 333. With introducing aspartic acid at the position 333, the block by Ca^{2+} was enhanced, suggesting that a negative charge at this position increases Ca^{2+} sensitivity. However, such enhancement was not observed with the introduction of glutamic acid. As for the block by La^{3+}, the block was not augmented by the introduction of glutamic acid (Fig. 1E). The effect of La^{3+} on N333D channel was not examined because the ATP-evoked current permeating through this channel became too small to analyze the blocking effect quantitatively in the presence of 1.8 mM Ca^{2+}, as seen in Fig. 1C.

Tests were made to determine the size-dependence found for the Ca^{2+} block was also found for the block by other divalent cations. Fig. 2A shows the block by Mg^{2+} of the

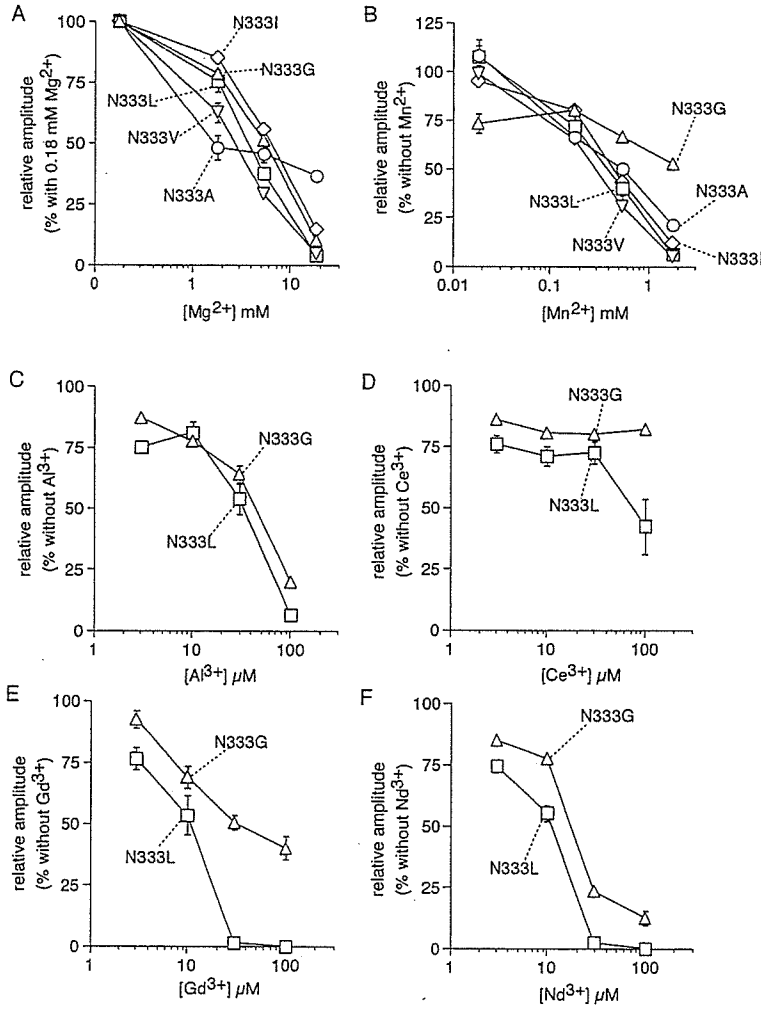

Fig. 2. Block by various multivalent cations of N333 neutral mutants. Current was measured as in Fig. 1A. Each symbol and bar represent the mean and S.E. obtained from four to five oocytes tested. (A, B) Concentration–response curve for Mg^{2+} (A) and Mn^{2+} block (B) on channels with neutral amino acid residues at the position 333. Current responses at −80 mV were normalized to those in the presence of 0.18 mM Mg^{2+} (A) or in the absence of Mn^{2+} (B). The normalized responses are plotted against the logarithm of Mg^{2+} or Mn^{2+} concentrations. The values from the statistical analysis of the block by 1.8 mM Mg^{2+} are $F=21.0$ ($P<0.001$ by ANOVA) and $P<0.001$ (N333A vs. N333L, N333A vs. N333G, N333A vs. N333I), $P<0.01$ (N333V vs. N333I), $P<0.05$ (N333A vs. N333V, N333V vs. N333I) or $P>0.05$ (N333V vs. N333L). (C–F) Effects of Al^{3+} (C), Ce^{3+} (D), Gd^{3+} (E) and Nd^{3+} (F) on N333G and N333L mutant channels. Current responses at −80 mV were normalized to those in the absence of trivalent cations. The normalized responses are plotted against the logarithm of trivalent cation concentrations.

neutral mutants of $P2X_2$ receptor/channel. When the magnitude of the block by 1.8 mM Mg^{2+} was compared, the block was apparently reduced in the order of Ala>Val>Leu>Gly>Ile. When statistically analyzed, the block by 1.8 mM Mg^{2+} with N333A was greater than with the remaining four mutants, and that with N333V was greater than with N333L, N333G or N333I. The results suggest that the size-dependence was found for the Mg^{2+} block except the Gly substitution. On the other hand, no size-dependence was found for the block by Mn^{2+} of these neutral mutants (Fig. 2B).

The effects of various trivalent cations were compared between N333G and N333L to determine whether or not selective block of N333G channel similar to that observed with La^{3+} was found. Among four trivalent cations tested (Al^{3+}, Ce^{3+}, Gd^{3+} and Nd^{3+}), none of them preferentially blocked N333G channel; the cations rather preferentially blocked N333L channel (Fig. 2C).

4. Discussion

By comparing the effects on the mutants possessing neutral amino acid residues at the position 333, we have demonstrated that the size of amino acid residues at this position affects the block by Ca^{2+} of $P2X_2$ receptor/channel. P2X receptor/channel in rat pheochromocytoma PC12 cells, the properties of which resemble those of the cloned $P2X_2$ receptor/channel, is permeable to both Na^+ and Ca^{2+}, but Ca^{2+} provides much smaller conductance than Na^+ does (Nakazawa and Hess, 1993). Ca^{2+} reduces net ionic current through the P2X receptor/channel by its competition with Na^+ at the channel pore. The block observed in the present study may mainly reflect this competitive inhibition. Thus, the size-dependence of the Ca^{2+} block indicates that larger amino acids at the channel pore mouth interferes with the access of Ca^{2+}. For the mutants with a negative charge at the position 333, N333D, but not N333E, exhibited higher sensitivity to Ca^{2+} than the wild type channel. This difference may due to a smaller size of aspartic acid residues than glutamic acid residues.

The selective block of the glycine-substituted mutant was also found for La^{3+}, but not for other multivalent cations tested, suggesting that the size-dependence is not uniform among cation species. One possible explanation for such diversity is the sizes of cations (or those of their hydrated forms). For example, the Shannon and Prett's ionic radius of Ca^{2+} is 1.14 Å at coordination number of 6, and this is larger than that of Mg^{2+} (0.86 Å) or Mn^{2+} (0.81 Å) (Cotton et al., 1995). Similarly, the ionic radius of La^{3+} of 1.06 Å is larger than those of other trivalent cations tested in the present study (Al^{3+} 0.68; Ce^{3+} 1.03; Gd^{3+} 0.94; Nd^{3+} 0.99; in Å). Large multivalent cations may be more readily affected by steric hindrance at the position 333.

In addition to size, negative polarity or charge at the position 333 is also a determinant of the magnitude of the Ca^{2+} block because, when comparing among amino acid residues of similar sizes (Val, Asn and Asp; Chothia, 1975), the sensitivity was increased according to negativity (Val < Asn < Asp; Fig. 1B and C). The sensitivity order of Val < Asn was also found for the block by Mg^{2+}, Mn^{2+} (not shown) and La^{3+} (Fig. 1D and E) and, thus, negative polarity at this position may attract multivalent cations regardless of cation species.

The present findings of the roles of the amino acid residue at the position 333 for multivalent cation block may further supports the importance of this position as the entrance of the channel pore, and may provide useful information about the relationship between the channel structure and functions including ion selectivity.

Acknowledgements

The authors are grateful to Profs. R. Alan Norh and Annmarie Surprenant for the supply of the mutant clones and helpful suggestions. This work was partly supported by a Health Science Research Grant for Research on Environmental Health and a "Nanomedicine" project grant from the Ministry of Health, Labour and Welfare, Japan, awarded to Y.O. and K.N., and a grant-in-aid for scientific research from the Ministry of Education, Science, Sports and Culture, Japan, awarded to K.N.

References

Arellano, R.O., Woodward, R.M., Miledi, R., 1995. A monovalent cationic conductance that is blocked by extracellular divalent cations in *Xenopus* oocytes. J. Physiol. 484, 593–604.

Brake, A.J., Wagenbach, M.J., Julius, D., 1994. New structural motif for ligand-gated ion channels defined by an ionotropic ATP receptor. Nature 371, 519–523.

Burnstock, G., 1997. The past, present, and future of purine nucleotides as signalling molecules. Neuropharmacology 36, 1127–1139.

Chothia, C., 1975. Structural invariants in protein folding. Nature 254, 304–308.

Cotton, F.A., Wilkinson, G., Gauss, P.L., 1995. Basic Organic Chemistry, 3rd ed. Wiley, New York, NY.

Ding, S., Sachs, F., 1999. Ion permeation and block of P2X(2) purinoceptors: single channel recordings. J. Membr. Biol. 172, 215–223.

Ding, S., Sachs, F., 2000. Inactivation of $P2X_2$ purinoceptors by divalent cations. J. Physiol. 522, 199–214.

Egan, T.M., Haines, W.R., Voigt, M.M., 1998. A domain contributing to the ion channel of ATP-gated $P2X_2$ receptors identified by the substituted cysteine accessibility method. J. Neurosci. 18, 2350–2359.

Haines, W.R., Voigt, M.M., Migita, K., Torres, G.E., Egan, T.M., 2001. On the contribution of the first transmembrane domain to whole-cell current through an ATP-gated ionotropic P2X receptor. J. Neurosci. 21, 5885–5892.

Jiang, L.H., Rassendren, F., Spelta, V., Surprenant, A., North, R.A., 2001. Amino acid residues involved in gating identified in the first membrane-spanning domain of the rat P2X(2) receptor. J. Biol. Chem. 276, 14902–14908.

Khah, B.S., 2001. Molecular physiology of P2X receptors and ATP signalling at synapses. Nat. Rev. 2, 165–174.

Migita, K., Haines, W.R., Voigt, M.M., Egan, T.M., 2001. Polar residues of the second transmembrane domain influence cation permeability of the ATP-gated P2X(2) receptor. J. Biol. Chem. 276, 30934–30941.

Nakazawa, K., Hess, P., 1993. Block by calcium of ATP-activated channels in pheochromocytoma cells. J. Gen. Physiol. 101, 377–392.

Nakazawa, K., Ohno, Y., 1996. Dopamine and 5-hydroxytryptamine selectively potentiate neuronal type ATP receptor channels. Eur. J. Pharmacol. 296, 119–122.

Nakazawa, K., Liu, M., Inoue, K., Ohno, Y., 1997. Potent inhibition by trivalent cations of ATP-gated channels. Eur. J. Pharmacol. 325, 237–243.

Nakazawa, K., Inoue, K., Ohno, Y., 1998a. An aspargine residue regulating conductance through $P2X_2$ receptor/channels. Eur. J. Pharmacol. 347, 141–144.

Nakazawa, K., Ohno, Y., Inoue, K., 1998b. An aspartic acid residue near the second transmembrane segment of ATP receptor/channel regulates agonist sensitivity. Biochem. Biophys. Res. Commun. 244, 599–603.

Negulyaev, Y.A., Markwardt, F., 2000. Block by extracellular Mg^{2+} of single human purinergic $P2X_4$ receptor channels expressed in human embryonic kidney cells. Neurosci. Lett. 279, 165–168.

North, R.A., Surprenant, A., 2000. Pharmacology of cloned P2X receptors. Annu. Rev. Pharmacol. Toxicol. 40, 563–580.

Rassendren, F., Buell, G., Newbolt, A., North, R.A., Surprenant, A., 1997. Identification of amino acid residues contributing to the pore of a P2X receptor. EMBO J. 16, 3446–3454.

Virginio, C., MacKenzie, A., Rassendren, F.A., North, R.A., Surprenant, A., 1999. Pore dilation of neuronal P2X receptor channels. Nat. Neurosci. 2, 315–321.

Zhang, Y., McBride Jr., D.W., Hamill, O.P., 1998. The ion selectivity of a membrane conductance inactivated by extracellular calcium in *Xenopus* oocytes. J. Physiol., 763–776.

TISSUE ENGINEERING
Volume 8, Number 3, 2002

Increase in Gap Junctional Intercellular Communication by High Molecular Weight Hyaluronic Acid Associated with Fibroblast Growth Factor 2 and Keratinocyte Growth Factor Production in Normal Human Dermal Fibroblasts

JEONG UNG PARK, Ph.D., and TOSHIE TSUCHIYA, Ph.D.

ABSTRACT

The effects of different molecular weights of hyaluronic acid (HA), a major component of extracellular matrix, on gap junctional intercellular communication (GJIC) in normal human dermal fibroblasts (NHDF cells) were investigated. NHDF cells were cultured for 4 days with different molecular weights of HA and then the extent of GJIC was assessed by the scrape-loading dye transfer method, using Lucifer yellow. The area of dye transfer was greater in the dishes coated with HA than in those to which HA was added. Thus, NHDF cells cultured on surfaces coated with high molecular weight (HMW) HA (MW, 800 kDa) showed greatly enhanced GJIC. Furthermore, another aim of this study was to evaluate the effects of different molecular weights of HA on the production of FGF-2 and KGF, because both are important cytokines produced by NHDF cells. When FGF-2 and KGF cultured levels of cell extracts and media were determined by ELISA, both levels were significantly enhanced when cells were grown on plates coated with HMW HA. This finding indicated that the function of gap junction channels in NHDF cells grown on plates coated with HMW HA may promote the biosynthesis of growth factors such as FGF-2 and KGF.

INTRODUCTION

MOST NORMAL CELLS within tissues have functional gap junctional intercellular communication (GJIC).[1,2] Gap junctions are constructed from transmembrane proteins that form structures called connexons. Gap junction channels are too small to enable the cell-to-cell passage of macromolecules such as proteins, and polysaccharides, but will allow free cell-to-cell diffusion of low molecular weight (LMW) molecules (<1 kDa). Consequently, many substances such as ions, water, sugars, nucleotides, amino acids, fatty acids, small peptides, drugs, and carcinogens are small enough to move between cells through gap junction channels.[3,4] Gap junction channels are important in coordinating the activities of electrically active cells, and they have been suggested to play a regulatory role in many processes, such as growth control, development and differentiation, synchronization, and metabolic regulation.[5–8]

The importance of GJIC makes it desirable to estimate gap junction channel function by a rapid and reliable quantitative method. The scrape-loading dye transfer (SLDT) method, involving use of the fluores-

Division of Medical Devices, National Institute of Health Sciences, Tokyo, Japan.

cent dye Lucifer yellow and published by Trosko et al. as a rapid and relatively uncomplicated method for measuring intercellular communication, has by now become a routine assay for analyzing the effects of various reagents on GJIC.[9]

Hyaluronic acid (HA) is a negatively charged glycosaminoglycan composed of repeated disaccharides of D-glucuronic acid and *N*-acetylglucosamine and is found in most types of extracellular matrix in the mammalian body.[10,11] By interaction with other matrix molecules, HA provides stability and elasticity to the extracellular matrix.[12–15] HA has been implicated in biological processes such as cell adhesion, migration, and proliferation. HA-binding proteins such as CD44, aggrecan, and versican have been implicated in structuring the extracellular matrix (ECM) by stabilizing large macromolecular aggregates. More importantly, Nagy et al. suggested that the receptor for HA-mediated motility (RHAMM) regulates gap junction channel and connexin-43 expression, possibly through its actions on focal adhesions and the associated cytoskeleton.[16] Neumann et al. also reported that HA can both promote and inhibit cytokine expression depending on its molecular mass.[17]

In a previous study, we showed that high molecular weight (HMW) HA promotes the function of gap junction channels in normal dermal fibroblasts (NHDF cells).[18] In fact, the size of HA and its application method are important factors in generating biocompatible tissue-engineered products, because the function of gap junction channels affects cell differentiation and the cell growth rate.[12,19,20]

Fibroblast growth factors (FGFs) play multiple roles during development and in adult tissues as paracrine regulators of growth and differentiation.[21] Furthermore, it was reported that stimulation of neurite growth correlated strongly with the amount of FGF-2 bound to surfaces coated with heparin, heparan sulfate, or HA.[22,23] Keratinocyte growth factor (KGF) is a member of the FGF family and is expressed almost exclusively by stromal cells from a variety of tissues, including the lung, skin, mammary gland, and prostate.[24] KGF *in vivo* is a member of the heparin-binding FGF family and is a paracrine mediator of proliferation and differentiation of a wide variety of epithelial cells. KGF has also been shown to cause angiogenesis and repair after major damage.[25,26]

The aim of the present study was to explore the relationship between gap junction channel function and production of growth factors. In the present study, we investigated the effect of LMW HA and HMW HA on FGF-2 and KGF expression by NHDF cells *in vitro*, and on gap junction channel function as estimated by the SLDT method, simultaneously.

MATERIALS AND METHODS

Materials

Lucifer yellow was purchased from Molecular Probes (Eugene, OR). AlamarBlue agent was obtained from Biosource (Camarillo, CA). Hyaluronic acids (HA, 800 kDa) were from Seikagaku Industries (Tokyo, Japan). HA of 4.8 kDa was prepared by the method of Cramer et al.[27] Quantikine, human FGF-2, and KGF immunoassay kits were from R&D Systems (Minneapolis, MN). All other special-grade chemicals were used without further purification.

Cell culture

Normal human dermal fibroblasts (NHDF cells; Asahi Techno Glass, Japan) were cultured in Dulbecco's modified Eagle's medium (DMEM; GIBCO-BRL, Bethesda, MD) supplemented with 10% heat-inactivated fetal calf serum (FBS; GIBCO-BRL) and antibiotics (penicillin [100 units/mL]–streptomycin [100 μg/mL]). NHDF cells were maintained in a humidified 5% CO_2 incubator at 37°C.

Preparation of culture dishes

Dishes used were 35-mm tissue culture polystyrene dishes (Asahi Techno Glass). HA polysaccharides were dissolved in distilled water at a concentration of 20 mg/mL. A 100-μL volume of HA solution was applied to each 35-mm dish. The HA-coated dishes were kept at room temperature for 2 days before use in SLDT and enzyme-linked immunosorbent assay (ELISA) experiments.

Scrape-loading dye transfer method

HA-coated 35-mm dishes were prepared as described in the preceding section. Cell monolayers were prepared as follows: 2 mL NHDF cell suspensions (1×10^5 cells/mL) were incorporated into control dishes (plastic dish group) and dishes coated with HA. In addition, cells were grown on plates for 4 h, after which HA was added. Assays were performed with confluent cultures that were obtained after 4 days of growth. Confluent NHDF cells were rinsed with phosphate-buffered saline containing Ca^{2+} and Mg^{2+} [PBS(+)] before addition of the fluorescent dye mixture (Lucifer yellow, MW 457.2). Lucifer yellow was added to the cells at a concentration of 0.1% and cut with a surgical blade at room temperature. The dye solution was left on the cells in a CO_2 incubator at 37°C for 5 min and then discarded, and the dishes were washed three times with PBS(+) to remove detached cells and background fluorescence. The extent of dye transfer was measured at room temperature under a fluorescence microscope, equipped with a type UFX-DXII CCD camera and super high-pressure mercury lamp power supply (Nikon, Tokyo, Japan). The images of the dye transfer were acquired by means of the UFG-DXII CCD camera. Measurement of the dye transfer was carried out 10 min after loading. Fluorescent areas were measured from digitized images by computation of the surface occupied by the dye.

FGF-2 and KGF assay by ELISA

Two hundred thousand NHDF cells were seeded onto 35-mm dishes. The conditioned medium was removed after 3 days of incubation and centrifuged at 1000 rpm for 2 min before washing with 0.5 mL of PBS(+). Cell suspensions were sonicated three times, each for 10 s, on ice. Both the conditioned medium and cell suspensions were stored at −20°C before assay. The FGF-2 and KGF levels of the cell-associated and supernatant samples were measured with commercially available ELISA kits.[28] Protein levels were quantified by comparing the optical density of each protein measured with its standard curve and normalizing for cell number.

RESULTS

The changes in gap junctional permeability induced by different molecular weights of HA were compared between the addition and coating methods (Figs. 1 and 2). Figure 1 shows fluorescent images of cells exposed to different molecular weights of HA. The images show that Lucifer yellow diffuses through gap junctions from loaded cells to neighboring cells. When NHDF cells were cultured on surfaces coated with

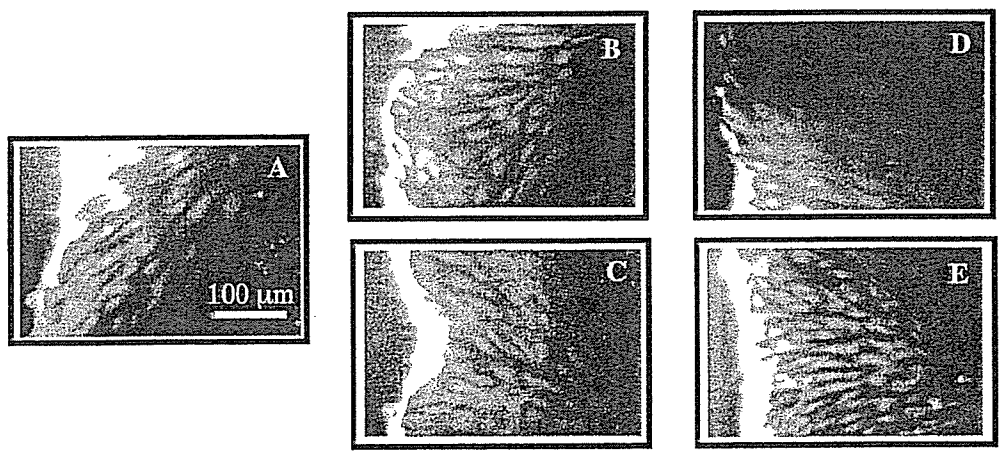

FIG. 1. Fluorescence images of cultured NHDF cells after scrape-loading with Lucifer yellow. **(A)** Control; **(B)** added–LMW HA (4.8 kDa); **(C)** coated–LMW HA (4.8 kDa); **(D)** added–HMW HA (800 kDa); **(E)** coated–HMW HA (800 kDa).

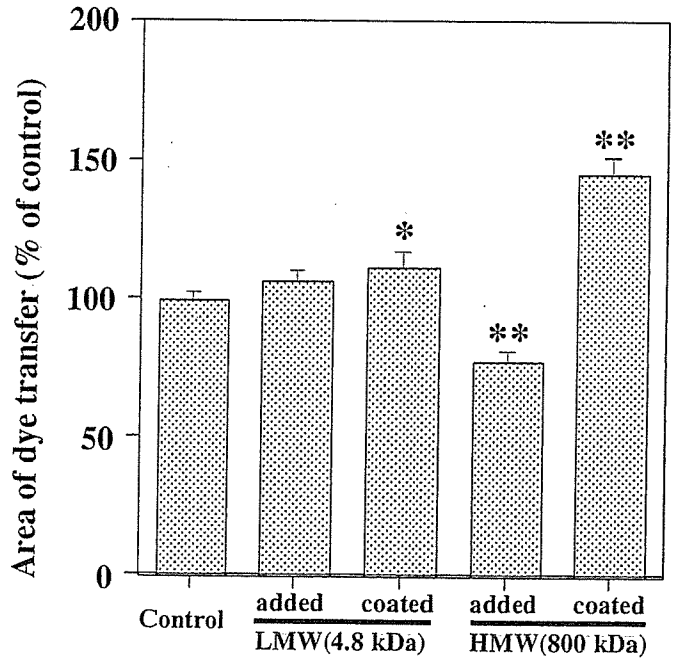

FIG. 2. Positive dye transfer by NHDF cells cultured on different added–HA and coated–HA dishes. $*p < 0.05$, $**p < 0.01$, added–HA and coated–HA groups versus control; Student t test.

HA, the fluorescent area based on the junctional permeability of Lucifer yellow generally increased between the cells. However, the dye transfer area was decreased when HMW HA (800 kDa) was added after 4 h of cell growth (i.e., added–HMW HA). Remarkably, the area of Lucifer yellow transfer in the coated–HMW HA plate was 1.5-fold higher than that of the control (Fig. 1E and Fig. 2). It seems to have been influenced by the affinities between HMW HA molecules and growth factors in the 10% FCS–DMEM. LMW HA only slightly enhanced the area of Lucifer yellow transfer, between 10 and 15%, under all conditions (Fig. 2).

Figure 3 shows the *in vitro* expression of FGF-2 in cell extracts and medium produced under coated–HA conditions. The total FGF-2 level in the presence of coated–HMW HA was higher than the control level. The trend toward an increased FGF-2 level was significantly correlated with the GJIC experimental findings, as shown in Fig. 1. The FGF-2 concentration in the cultured cell medium was about 0.1% of that in the cell extract, and cells in the presence of coated–HMW HA contained a lower medium level of FGF-2 than did the medium of other cultures.

Figure 4 shows *in vitro* production of KGF in cell extracts and medium produced under coated–HA conditions. The total KGF level produced under coated–HMW HA conditions was also about 30% higher than the control level, while that produced under coated–LMW HA conditions was reduced. This strongly indicates that KGFs are produced by natural HA- and HMW HA-enriched pericellular matrices. The KGF concentrations in the cultured cell medium did not change under any condition (Fig. 4B).

DISCUSSION

The most abundant macromolecules in cartilage are HA, collagen, aggrecan, and link protein, which are believed to play roles in maintaining a unique three-dimensional network for a functional joint. HA is a major glycosaminoglycan that is synthesized by human skin fibroblasts and has the intrinsic ability to promote cell proliferation and reduce scar formation.[29,30] This study demonstrated that coated–HMW HA conditions increased GJIC among NHDF cells and upregulated the expression of FGF-2 and KGF. In our study

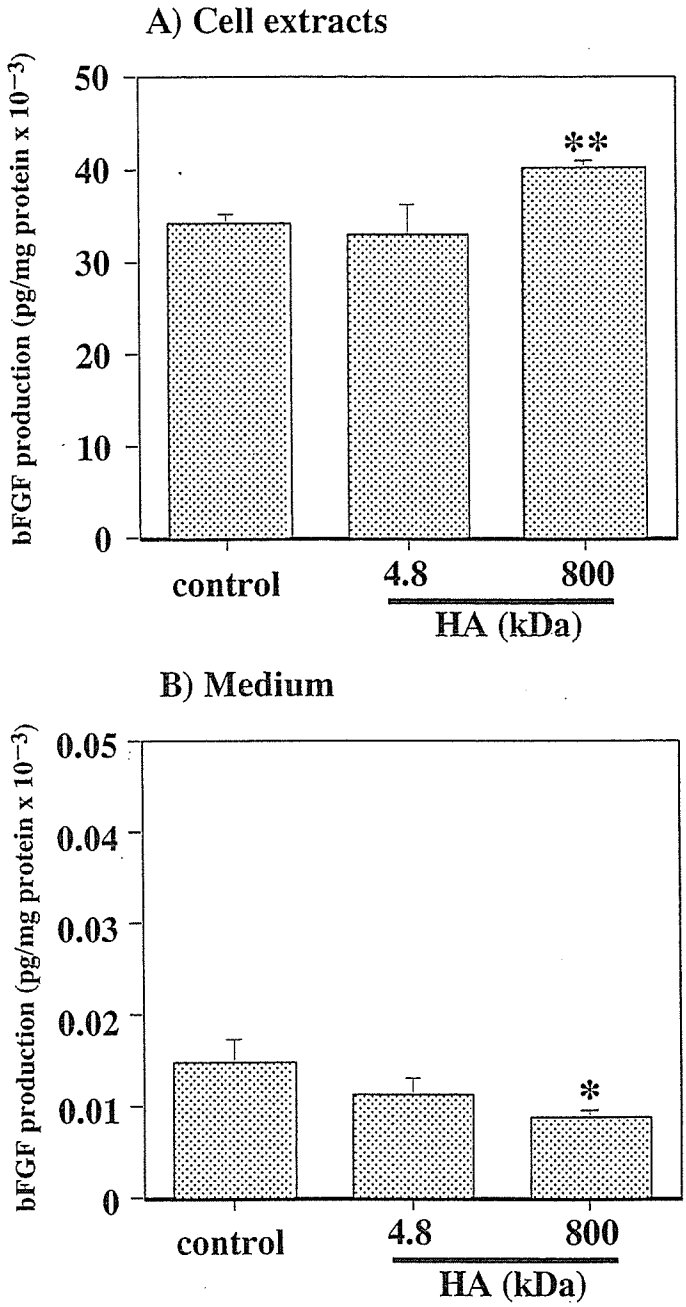

FIG. 3. FGF-2 level measured by ELISA of NHDF cells cultured for 4 days on plates coated with HA. (**A**) FGF-2 level in cell extracts; (**B**) FGF-2 level in cell culture medium. $*p < 0.05$, $**p < 0.01$, samples versus control; Student *t* test.

of the effects of HA on GJIC of NHDF cells, NHDF cells grown under coated–HMW HA conditions caused promotion of GJIC, but not under added–HMW HA conditions. However, LMW HA produced a slightly greater area of dye transfer than in untreated controls, whether the LMW HA was coated on the plate or added later. These differences were thought to be caused by different abilities to form three-dimensional structures, which probably involves growth factors, etc.[31–33] In another study,[18] we report that the increase in dye transfer is thought to be related to the affinities between HMW HA molecules and growth factors

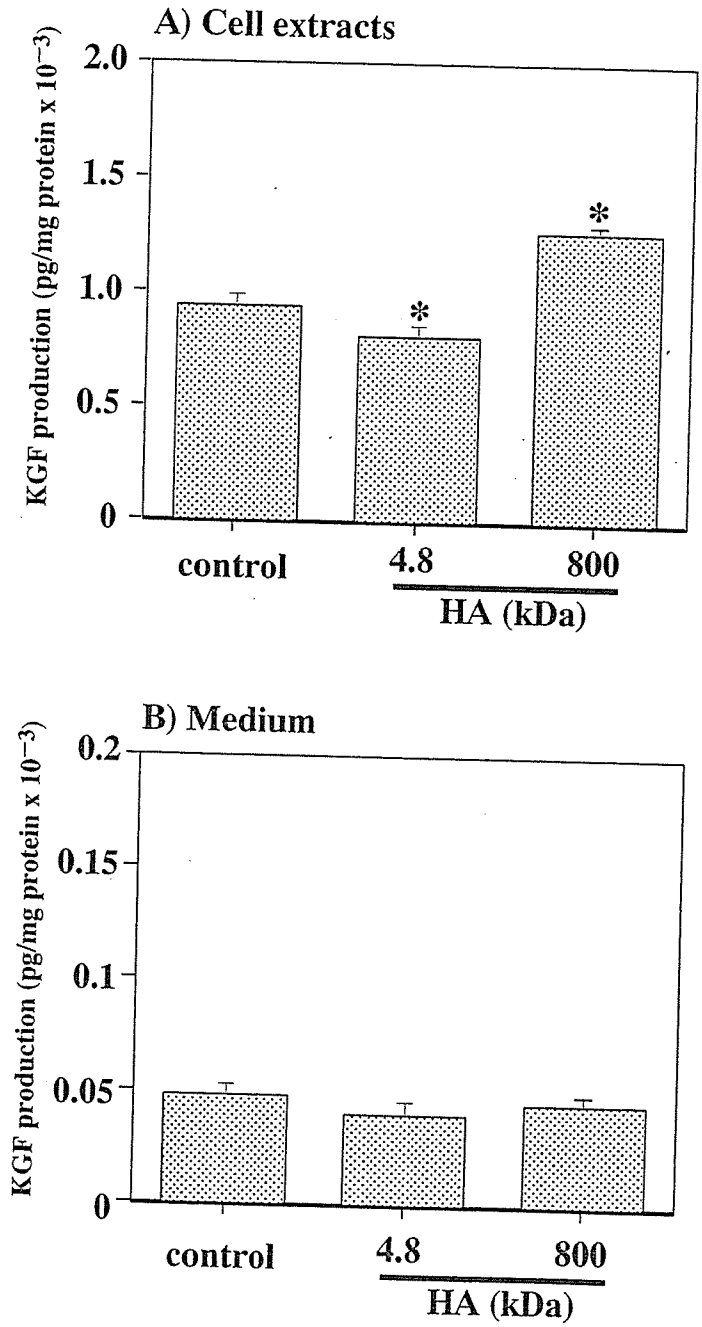

FIG. 4. KGF level measured by ELISA of NHDF cells cultured for 4 days on plates coated with HA. (**A**) KGF level in cell extracts; (B) KGF level in cell culture medium. $*p < 0.05$, samples versus control; Student t test.

in the 10% FCS–DMEM (data not shown). Thus, it was suggested that the HMW HA-coated surface provides a stable anionic surface that prevents cell attachment during the early stage of growth.[34] Consequently, these findings suggested that the junctional permeability for Lucifer yellow in NHDF cells was significantly enhanced only when NHDF cells were cultured on HMW HA-coated surfaces.[35,36]

The dye transfer between NHDF cells was dependent on HA molecular size and stimulated by coated–HA conditions. In particular, we analyzed the diffusion area of the dye on the basis of the intensity of fluores-

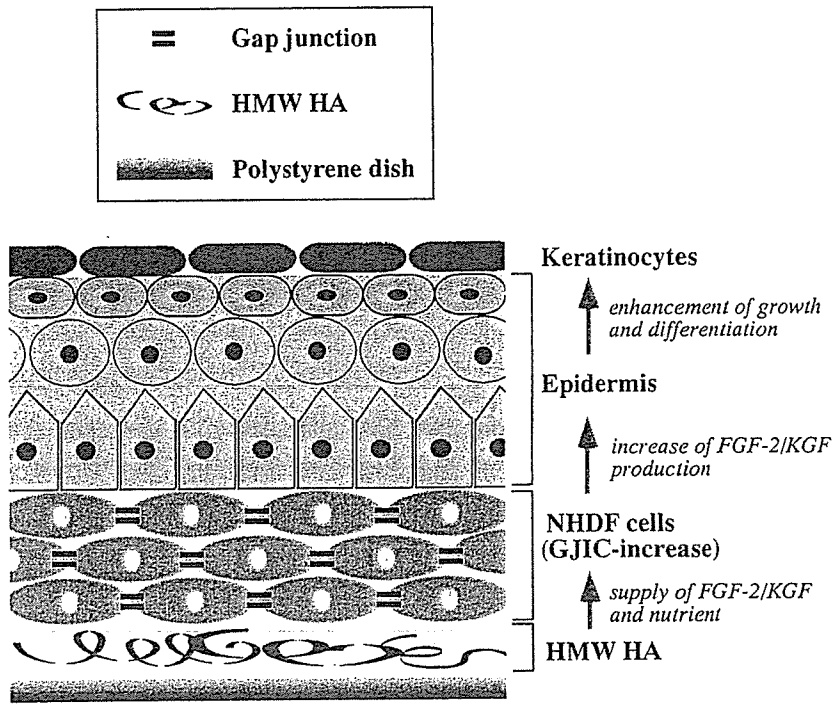

FIG. 5. Model of artificial skin demonstrating the effects of GJIC increase in NHDF cells by HMW HA.

cence. This method makes it possible to estimate GJIC function more precisely than that estimated by the dye migration distance in an earlier study.[37,38]

As expected, we showed that the activities of FGF-2 and KGF were strongly related to GJIC of NHDF cells cultured in HA-coated dishes.[39–41] When various molecular weights of HA were compared, cells grown on HMW HA produced more FGF-2 and KGF than did cells grown on LMW HA. The relationship between FGF-2 expression and GJIC paralleled well the observations of Nadarajah et al., who reported that FGF-2 increases the expression of gap junction protein connexin 43 and its mRNA.[42] Thus, FGF-2 and KGF production correlated well with the extent of GJIC function of NHDF cells cultured on surfaces coated with HMW HA. Similarly, Isakson et al. demonstrated that rat alveolar type II cells cultured in KGF showed increased expression of connexin.[43]

From these findings, nutrients that promote the formation of gap junctions, such as FGF-2 and KGF, could be enveloped in HMW HA molecules coated on dishes, and these cytokines are well known to stimulate the growth and differentiation of epidermis to keratinocytes. Therefore, we believe that this system may improve GJIC in artificial skin as well as enhance the production of growth factors, such as FGF-2 and KGF, by NHDF cells (Fig. 5).

REFERENCES

1. Abdullah, K.M., Luthra, G., Bilski, J.J., Abdullah, A., Reynolds, L.P., Redmer, D.A., and Grazul-Bilska, A.T. Cell-to-cell communication and expression of gap junctional proteins in human diabetic and nondiabetic skin fibroblasts. Endocrine **10,** 35, 1999.
2. Grossman, H.B., Liebert, M., Lee, I.W., and Lee, S.W. Decreased connexin expression and intercellular communication in human bladder cancer cells. Cancer Res. **54,** 3062, 1994.
3. Vera, B., Sanchez-Abarca, L.I., Bolanos, J.P., and Medina, J.M. Inhibition of astrocyte gap junctional communication by ATP depletion is reversed by calcium sequestration. FEBS Lett. **392,** 225, 1996.
4. Bukauskas, F., Jordan, K., Bukauskiene, A., Bennett, M.V., Lampe, P.D., Laird, D.W., and Verselis, V. Cluster-

ing of connexin 43-enhanced green fluorescent protein gap junction channels and functional coupling in living cells. Proc. Natl. Acad. Sci. U.S.A. **97,** 2556, 2000.

5. Giaume, C., Marin, P., Cordier, J., Glowinski, J., and Premont, J. Adrenergic regulation of intercellular communications between cultured striatal astrocytes from the mouse. Proc. Natl. Acad. Sci. U.S.A. **88,** 5577, 1991.
6. Upham, B.L., Yao, J.J., Trosko, J.E., and Masten, S.J. Determination of the efficacy of ozone treatment systems using a gap junction intercellular communication bioassay. Environ. Sci. Technol. **29,** 2923, 1995.
7. Warn-Cramer, B.J., Cottrell, G.T., Burt, J.M., and Lau, A.F. Regulation of connexin-43 gap junctional intercellular communication by mitogen-activated protein kinases. J. Biol. Chem. **273,** 9188, 1998.
8. Tsuchiya, T. A useful marker for evaluating tissue-engineered products: gap-junctional communication for assessment of the tumor-promoting in tissue-engineering products. J. Biomater. Sci. Polym. Ed. **11,** 947, 2000.
9. Trosko, J.E., Madhukar, B.V., and Chang, C.C. Endogenous and exogenous modulation of gap junctional intercellular communication: toxicological and pharmacological implications. Life Sci. **53,** 1, 1993.
10. Lapcik, L., Jr., Lapcik, L., Smedt, S.D., Demeester, J., and Chabrecek, P. Hyaluronan: preparation, structure, properties, and applications. Chem. Rev. **98,** 2663, 1998.
11. Laurent, T.C., and Fraser, J.E. Hyaluronan. FASEB J. **6,** 2397, 1992.
12. Cowman, M.K., Li, M., and Balazs, E.A. Tapping mode atomic force microscopy of hyaluronan: Extended and intramolecularly interacting chains. Biophys. J. **75,** 2030, 1998.
13. Greco, R.M., Iocono, J.A.., and Ehrlich, H.P. Hyaluronic acid stimulates human fibroblast proliferation within a collagen matrix. J. Cell. Phys. **177,** 465, 1998.
14. Culty, M., Nguyen, H.A., and Underhill, C.B. The hyaluronan receptor (CD44) participates in the uptake and degradation of hyaluronan. J. Cell Biol. **116,** 1055, 1992.
15. Heldin, P., Laurent, T.C., and Heldin, C.H. Effect of growth factors on hyaluronan synthesis in cultured human fibroblasts. Biochem. J. **258,** 919, 1989.
16. Nagy, J.I., Hossain, M.Z., Lynn, B.D., Curpen, G.E., Yang, S., and Turley, E.A. Increased connexin-43 and gap junctional communication correlates with altered phenotypic characteristics of cells overexpressing the receptor for hyaluronic acid-mediated motility. Cell Growth Differ. **7,** 745, 1996.
17. Neumann, A., Schinzel, R., Riederer, P.D., and Munch, G. High molecular weight hyaluronan inhibits advanced glycation endproduct-induced NF-κB activation and cytokine expression. FEBS Lett. **25,** 283, 1999.
18. Park, J.U., and Tsuchiya, T. In vitro safety evaluation of hyaluronic acids for bioartificial organs: increase in gap-junctional intercellular communications (GJIC) of normal human dermal fibroblasts (NHDF) on surfaces coated with high molecular weight hyaluronic acid (HMW HA). J. Biomed. Mater. Res. **60,** 541, 2002.
19. Henrich, C.J., and Hawkes, S.P. Molecular weight dependence of hyaluronic acid produced during oncogenic transformation. Cancer Biochem. Biophys. **10,** 257, 1989.
20. Sasaki, T., and Watanabe, C. Stimulation of osteoinduction in bone wound healing by high-molecular-weight hyaluronic acid. Bone **16,** 9, 1995.
21. Plotnikov, A., Schlessinger, J., Hubbard, S., and Mohammad, M. Structural basis for FGF receptor dimerization and activation. Cell **98,** 641, 1999.
22. Relou, I.A., Damen, C.A., van der Schaft, D.W., Groenewegen, G., and Griffioen, A.W. Effect of culture conditions on endothelial cell growth and responsiveness. Tissue Cell **30,** 525, 1998.
23. Walicke, P.A. Interactions between basic fibroblast growth factor (FGF) and glycosoaminoglycans in promoting neurite outgrowth. Exp. Neurol. **102,** 144, 1988.
24. Bloome, E.G., Sugimoto, Y., Lin, Y.C., Capen, C.C., and Rosel, T.J. Parathyroid hormone-related protein is a positive regulator of keratinocyte growth factor expression by normal dermal fibroblasts. Mol. Cell. Endocrinol. **152,** 189, 1999.
25. Gillis, P., Savla, U., Volpert, O.V., Jimenez, B., Waters, C.M., Panos, R.J., and Bouck, N.P. Keratinocyte growth factor induces angiogenesis and protects endothelial barrier function. J. Cell Sci. **112,** 2049, 1999.
26. Abraham, V., Cho, M.L., DeBolt, K.M., and Koval, M. Phenotype control of gap junctional communication by cultured alveolar epithelial cells. Am. J. Physiol. **276,** L825, 1999.
27. Cramer, J.A., Bailey, L.C., Bailey, C.A., and Miller, R.T. Kinetic and mechanistic studies with bovine testicular hyaluronidase. Biochim. Biophys. Acta **1200,** 315, 1993.
28. Ulich, T.R., Whitcomb, L., Tang, W., Tressel, P.C., Tarpley, J., Yi, E.S., and Lacay, D. Keratinocyte growth factor ameliorates cyclophosphamide-induced ulcerative hemorrhagic cystitis. Cancer Res. **57,** 472, 1997.
29. Lisignoli G., Zini N., Remiddi G., Piacentini A., Puggioli A., Trimarchi C., Fini M., Maraldi N.M., and Facchini A. Basic fibroblast growth factor enhances in vitro mineralization of rat bone marrow stromal cells grown on non-woven hyaluronic acid based polymer scaffold. Biomaterials **22,** 2095, 2001.
30. Hu, M., Sabelman, E.E., Tsai, J., and Hentz, V.R. Improvement of Schwann cell attachment and proliferation on modified hyaluronic acid strands by polylysine. Tissue Eng. **6,** 585, 2000.

31. Calvo, J.C., Gandjbakhche, A.H., Nossal, R., Hascall, V.C., and Yanagishita, M. Rheological effects of the presence of hyaluronic acid in the extracellular media of differentiated 3T3-L1 preadipocyte cultures. Arch. Biochem. Biophys. **302,** 468, 1993.
32. Toole, B.P. Hyaluronan in morphogenesis. J. Intern. Med. **242,** 35, 1997.
33. Nakamura, T., Takagaki, K., Kubo, K., Morikawa, A., Tamura, S., and Endo, M. Extracellular depolymerization of hyaluronic acid in cultured human skin fibroblasts. Biochem. Biophys. Res. Commun. **172,** 70, 1990.
34. Eitle, T., Keler, T., Parish, C.R., and Parish, R.W. Polysaccharides influence the aggregation of *Dictyostelium discoideum* cells and bind to developmentally regulated cell surface proteins. Exp. Cell Res. **205,** 374, 1993.
35. Bost, F., Diarra-Mehrpour, M., and Martin, J.P. Inter-α-trypsin inhibitor proteoglycan family a group of proteins binding and stabilizing the extracellular matrix. Eur. J. Biochem. **252,** 339, 1998.
36. Kawasaki, K., Ochi, M., Uchio, Y., Adachi, N., and Matsusaki, M. Hyaluronic acid enhances proliferation and chondroitin sulfate synthesis in cultured chondrocytes embedded in collagen gels. J. Cell. Phys. **179,** 142, 1999.
37. Opsahl, H., and Rivedal, E. Quantitative determination of gap junction intercellular communication by scrape loading and image analysis. Cell Adhes. Commun. **7,** 367, 2000.
38. Kavanagh, T.J., Martin, G.M., El-fouly, M.H., Trosko, J.F., Chang, C.C., and Rabinovitch, P.S. Flow cytometry and scrape-loading/dye transfer as a rapid quantitative measure of intercellular communication in vitro. Cancer Res. **47,** 6046, 1987.
39. Pepper, M.S., and Meda, P. Basic fibroblast growth factor increases junctional communication and connexin 43 expression in microvascular endothelial cells. J. Cell Physiol. **153,** 196, 1992.
40. Salmivirta, M., Heino, J., and Jalkanen, M. Basic fibroblast growth factor–syndecan complex at cell surface or immobilized to matrix promotes cell growth. J. Biol. Chem. **267,** 17606, 1992.
41. Pedro, T.D., Paloma, R.S., Beatriz, M.C., and Javier, D.G. bFGF stimulates GAP-43 phosphorylation at Ser41 and modifies its intercellular localization in cultured hippocampal neurons. Mol. Cell. Neurosci. **16,** 766, 2000.
42. Nadarajah, B., Makarenkova, H., Becker, D.L., Evans, W.H., and Parnavelas, G. Basic FGF increases communication between cells of the developing neocortex. I. Neuroscience **18,** 7881, 1998.
43. Isakson, B.E., Lubman, R.L., Seedorf, G.J., and Boitane, S. Modulation of pulmonary alveolar type II cell phenotype and communication by extracellular matrix and KGF. Am. J. Physiol. **281,** C1291, 2001.

Address reprint requests to:
Toshie Tsuchiya, Ph.D.
Division of Medical Devices
National Institute of Health Sciences
1-18-1, Kamiyoga, Setagaya-ku
Tokyo 158-8501, Japan

E-mail: tsuchiya@nihs.go.jp

Increase in gap-junctional intercellular communications (GJIC) of normal human dermal fibroblasts (NHDF) on surfaces coated with high-molecular-weight hyaluronic acid (HMW HA)

Jeong Ung Park, Toshie Tsuchiya
Division of Medical Devices, National Institute of Health Sciences, Kamiyoga, 1-18-1, Setagaya-ku, Tokyo, 158-8501, Japan

Received 2 March 2001; accepted 11 May 2001
Published online 7 March 2002 in Wiley InterScience (www.interscience.wiley.com). DOI: 10.1002/jbm.10171

Abstract: Normal human dermal fibroblast (NHDF) cells were used to detect differences in gap-junctional intercellular communication (GJIC) by hyaluronic acid (HA), a linear polymer built from repeating disaccharide units that consist of N-acetyl-D-glucosamine (GlcNa) and D-glucuronic acid (GlcA) linked by a β1-4 glycosidic bond. The NHDF cells were cultured with different molecular weights (MW) of HA for 4 days. The rates of cell attachment in dishes coated with high-molecular-weight (HMW; 310 kDa or 800 kDa) HA at 2 mg/dish were significantly reduced at an early time point compared with low-molecular-weight (LMW; 4.8 kDa or 48 kDa) HA with the same coating amounts. HA-coated surfaces were observed by atomic force microscopy (AFM) under air and showed that HA molecules ran parallel in the dish coated with LMW HA and had an aggregated island structure in the dish coated with HMW HA surfaces. The cell functions of GJIC were assayed by a scrape-loading dye transfer (SLDT) method using a dye solution of Lucifer yellow. Promotion of the dye transfer was clearly obtained in the cell monolayer grown on the surface coated with HMW HA. These results suggest that HMW HA promotes the function of GJIC in NHDF cells. In contrast, when HMW HA was added to the monolayer of NHDF cells, the functions of GJIC clearly were lowered in comparison with the cells grown in the control dish or with those grown on the surface of HMW HA. Therefore it is concluded that the MW size of HA and its application method are important factors for generating biocompatible tissue-engineered products because of the manner in which the GJIC participates in cell differentiation and cell growth rate. © 2002 Wiley Periodicals, Inc. J Biomed Mater Res 60: 541–547, 2002

Key words: hyaluronic acid; normal human dermal fibroblast; gap junctional intercellular communication; scrape loading and dye transfer; atomic force microscopy

INTRODUCTION

Normal cells and tissues have functional gap junctions. Gap junctions—hydrophilic intercellular channels that allow intercellular passage of small molecules (up to 1 kDa)—are constructed from connexin proteins that form structures called connexons. Moreover, many substances, such as ions, sugars, nucleotides, amino acids, drugs, carcinogens, et al., are small enough to move between cells though gap-junction channels. Gap junctions are important for coordinating the activities of electrically active cells, and they are thought to play many regulatory roles, such as growth control, developmental and differentiation processes, synchronization, and metabolic regulation.

Correspondence to: T. Tsuchiya; e-mail: tsuchiya@nihs.go.jp

The aim of the present study was to clarify the effect of hyaluronic acid (HA) on intercellular communication via gap junction.

Many investigators have demonstrated increases in cell migration, invasion, and proliferation by exposure to HA.[1,2] Kawasaki et al. also have reported that HA in collagen gel culture enhanced the proliferation and chondroitin 6-sulfate synthesis of chondrocytes while maintaining their phenotype.[3] HA is involved in these processes via cell–surface receptors, such as the receptor for HA-mediated motility (RHAMM) and CD44 glycoproteins. Additionally, cellular behaviors such as adhesion, differentiation, and proliferation were greatly affected by surface properties such as receptor–ligand binding, hydrophilicity, roughness, charge, and morphology of the materials. In this study, safety evaluation for HA was investigated using NHDF cells, which are known to express CD44 glycoproteins on their surface.[4]

In tissue engineering, it is not known if HA is an important component, so we investigated the effects of HA on the gap-junctional intercellular communication (GJIC) function of NHDF cells.[5–9] Furthermore, the technique of AFM was used in this study on the surface structure of various molecular weights (MW) of HA.[10,11] The present paper reports that the HA structures of various MW are related to the control of cell functions.

MATERIALS AND METHODS

Materials

Lucifer yellow was purchased from Molecular Probes (Eugene, OR). AlamarBlue™ agent was purchased from Biosource (Camarillo, CA). Giemsa's solution was obtained from Merck (Germany). Hyaluronic acids (HA: 48 kDa, 300 kDa, and 800 kDa) kindly were supplied by Seikagaku Industries, Ltd. (Tokyo, Japan). HA of 4.8 kDa was prepared using the method of Cramer and co-workers.[12] All other chemicals of a special grade were used without further purification.

Cell culture

Normal human dermal fibroblasts (NHDF) cells (Asahi Techno Glass, Tokyo, Japan) were cultured in Dulbecco's modified Eagle's medium (DMEM; GIBCO BRL) supplemented with 10% heat-inactivated fetal calf serum (FCS; GIBCO BRL) and antibiotics [penicillin (100 unit/mL)–streptomycin (100 μg/mL)]. NHDF cells in DMEM–10% FCS medium were maintained in a humidified 5% CO_2 incubator at 37°C. The cells were allowed to form a fully confluent monolayer.

Preparation of culture dishes

The dishes used were 35-mm polystyrene dishes (Falcon 1008, Becton Dickinson). The HA polysaccharides were dissolved in distilled water at a concentration of 20 mg/mL. Each 35-mm culture dish was coated or added into each well after 4 h of culture at a final concentration of 2 mg/dish. The HA-coated dishes were dried further under sterile air flow at room temperature for 24 h before use.

Atomic force microscopy (AFM)

For AFM studies, HA-coated dishes were prepared as described above. HA-coated dish surfaces were visualized by an atomic force microscope (Nanoscope III; Digital Instrument, Santa Barbara, CA). Images were obtained by scanning the surface in a tapping mode using Nanoprobe™ SPM tips.

Cell viability

For measurement of cell viability, 8×10^4 NHDF cells were seeded into HA-added, or -coated 12-well plastic dishes. Solutions of various molecular weights of HA were added (HA 2 mg/mL, 1 mL/dish) or coated (2 mg/dish) in the same amounts of HA per dish for SLDT analysis. After 4 days of HA treatment, the extent of cell viability was measured by alamarBlue™ assay.[13] Control cells received fresh medium without any additions.

Cell adhesion assay in HA-coated dishes

HA-coated dishes were prepared as described above. Two mL of NHDF cell suspension (1×10^5/mL) were added onto each substratum-coated culture dish. Dishes were incubated for 4, 24, and 72 h, respectively. For cell adhesion assay, the cells were fixed and stained with Giemsa's solution and observed by an optical microscope.

Scrape-loading and dye transfer (SLDT) analysis

NHDF cells were incorporated at very high densities into the HA-coated dishes and allowed to form a fully confluent monolayer. The cell monolayer was rinsed thee times with PBS (+) before the addition of the fluorescent dye (Lucifer yellow: MW 457.2). The cell monolayer was scraped using a surgical blade and loaded with 0.1% Lucifer yellow solution. The dye solution was left on the cells, and the cells were incubated at 37°C for 5 min in a humidified atmosphere containing 5% CO_2 and 95% air. The dye solution was discarded from 35-mm^2 plastic Petri dishes, and the dishes were washed thee times with 1 mL of PBS (+) solution to remove detached cells and background fluorescence. The distance of dye migration was measured at room temperature under the fluorescence microscope equipped with a type UFX-DXII and Super High Pressure Mercury Lamp Power Supply (NIKON, Japan). Measurement was carried out within 10 min after dye-loading.

RESULTS AND DISCUSSION

At the same amounts of HA (2 mg/dish), attachment of NHDF cells to HMW HA was significantly less at an early time point than it was to LMW HA. Figure 1 shows the appearance of the attachment of NHDF cells in the dishes coated with four different MW of HA. After 24 h, the cells in the LMW HA-

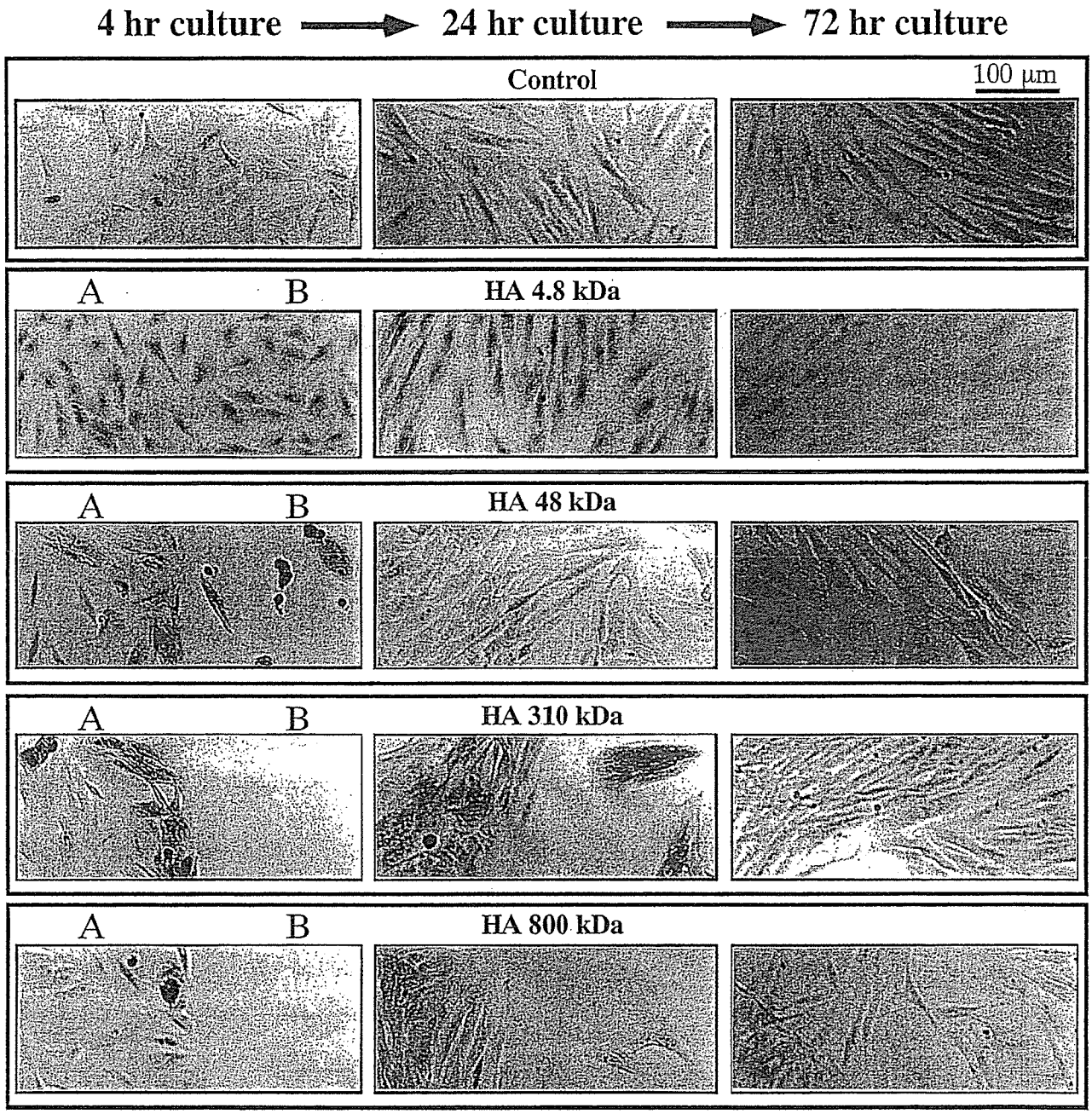

Figure 1. NHDF cell adhesion to the polystyrene dishes half coated with various HA: (A) uncoated portion, and (B) coated portion of HA.

coated dishes (HA 4.8 kDa and 48 kDa) already had attached and were confluent. By contrast, the HMW HA-coated dishes (HA 310 kDa and 800 kDa) had low adhesiveness to the cells. It has been suggested that the HMW HA-coated surface provides a stable anionic surface that prevents cell attachment at the early time point, as shown in Figure 2(B).[14] The difference in cell attachment activity may depend on the surface structure of the coated HA.

To investigate the relationship between the morphology of HA-coated dishes and cell attachment, the surfaces of the dishes were examined by tapping mode AFM. Different surface appearances were observed in various MW HA-coated polystyrene dishes (Fig. 2). Figure 2 is an AFM phase image of an 80 × 80-nm area under air. The control polystyrene surface is shown in Figure 2(A) [see (a)]. The dish surface coated with LMW HA was relatively smooth [see (b) in Fig. 2(A) and (a) in Fig. 2(B)]. In contrast, on the HMW HA surfaces, an island-shaped structure was observed [see (d) in Fig. 2(A) and (b) in Fig. 2(B)].

These phenomena probably are due to the intramolecular association of HMW HA.[15] Our images indicate that intramolecular association between long HA

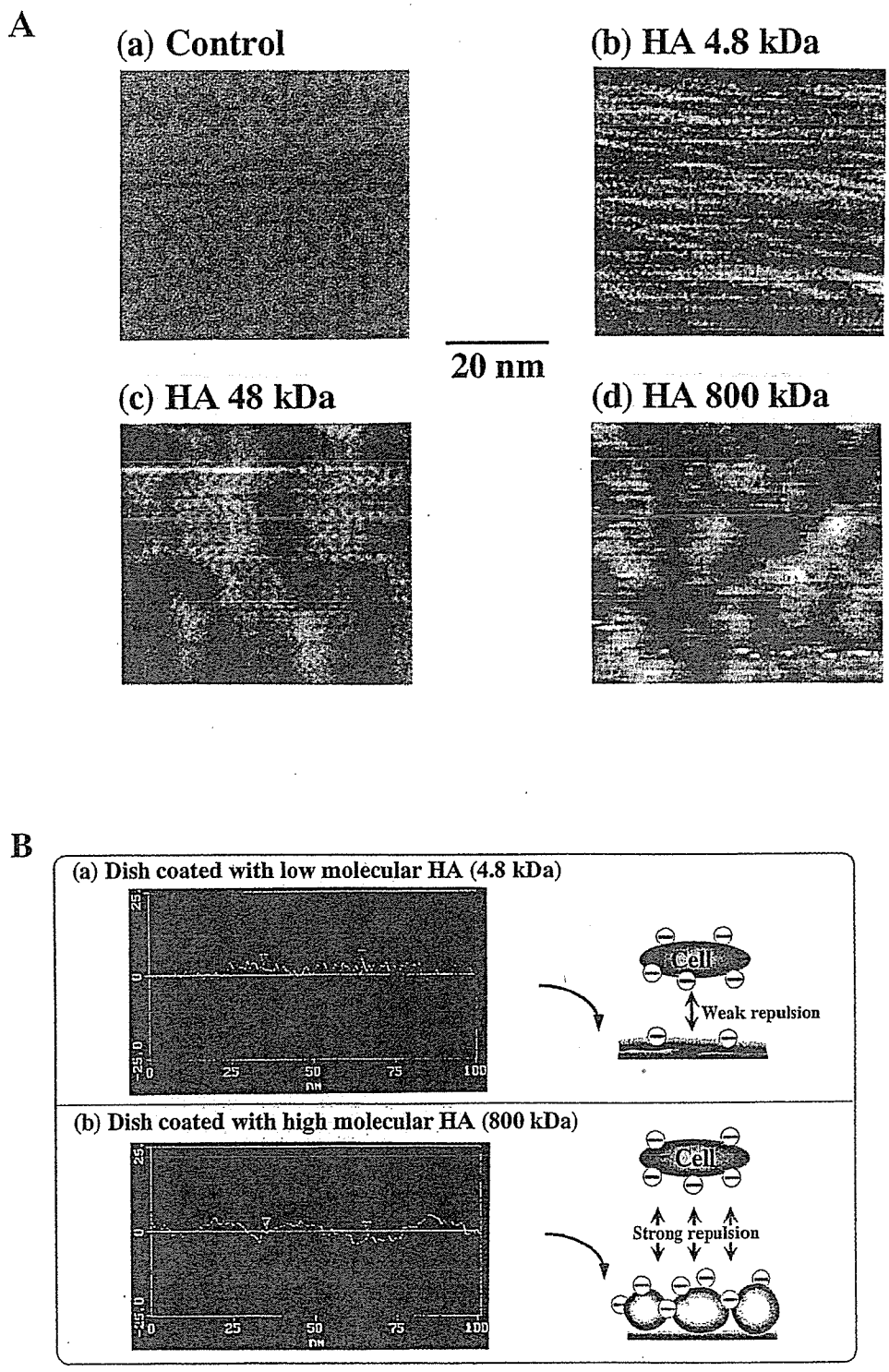

Figure 2. AFM images of polystyrene dish surfaces coated with various HA: (A) AFM images by phase mode; and (B) AFM section analysis and schematic diagrams of interaction between HA-coated dishes and cells.

chains results in the formation of island structures. Many islands composed of 800 kDa MW HA also clearly were observed, and the island size was about 20 nm wide and 10 nm high [see (b) in Fig. 2(B)].

The negative charge of the HA molecules is another important aspect in understanding biologic properties in interaction with the cells. Thus the surface charge by carboxylic groups (–COOH) of HA molecules may cause a decrease in cell attachment activity in the 310 kDa and the 800 kDa of HA MW at an early time point (Fig. 1). However, the cells were completely attached and grown to confluency over 4 days of culture while HA added in medium had no significant effect on rates of cell attachment (data not shown).

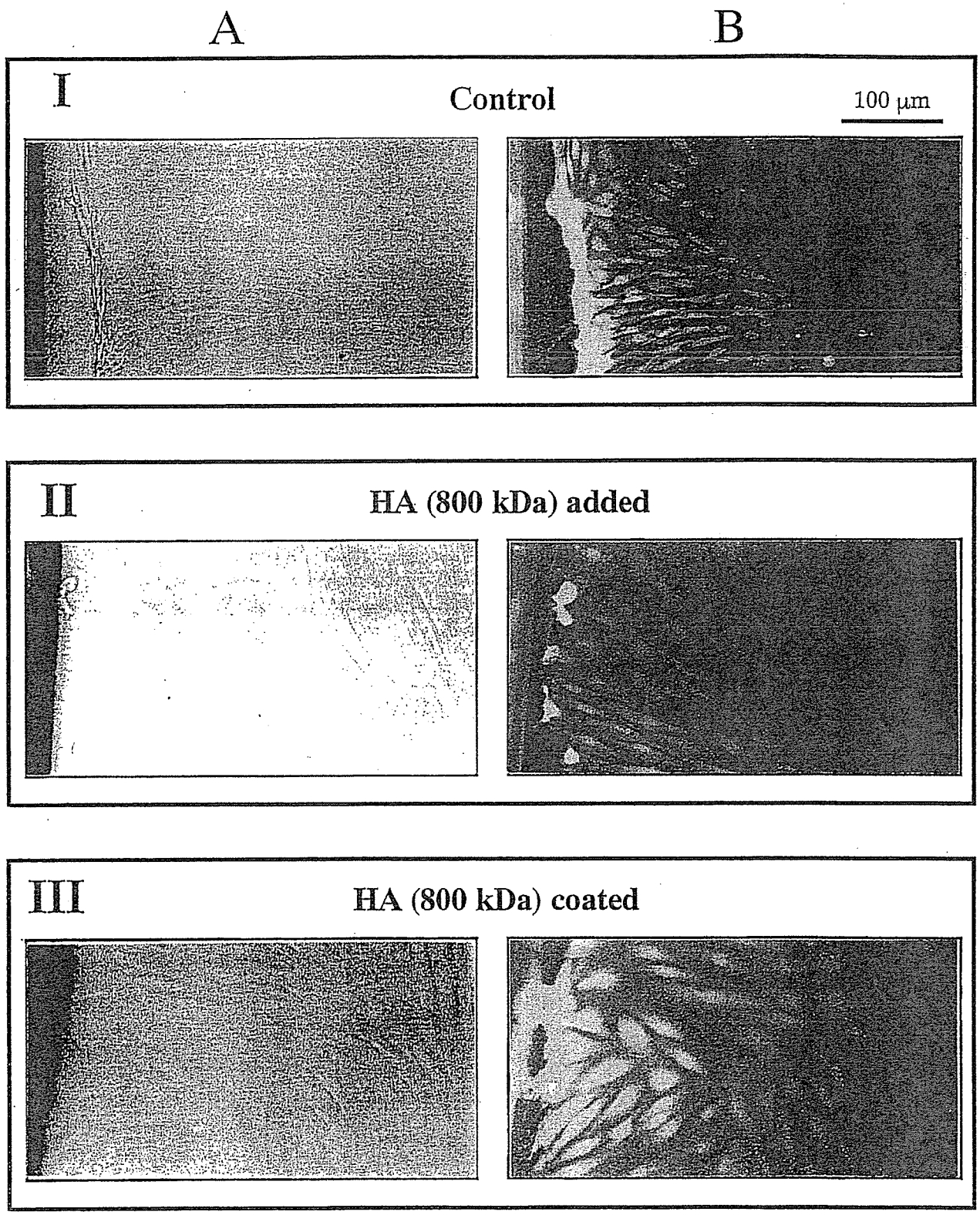

Figure 3. Positive dye transfer of NHDF cells cultured with HA (800 kDa)-added, or coated dishes: (A) phase-contrast photomicrographs of NHDF cells after scrape-loading in the presence of Lucifer yellow; and (B) epifluorescence photomicrographs of scrape-loading and dye transfer correspond to the same fields.

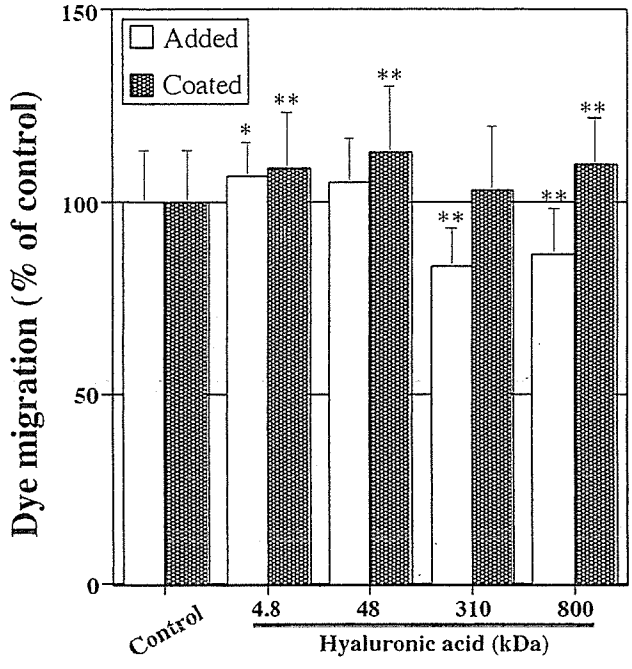

Figure 4. Dye transfer ratio of NHDF cells cultured with various HA (*$P < 0.5$, **$P < 0.01$, samples vs. control in added or coated group).

Assessment of GJIC function was performed by SLDT assay using Lucifer yellow. With cell culture for 4 days in HA-added or coated dishes, the cells were strongly attached to the dish and grown to confluency, and the GJIC function was surveyed. By making a scrape line in the culture using a surgical blade, the fluorescent dye penetrated the adjacent cells. Figure 3 shows patterns of dye migration in NHDF cells treated with HMW HA (800 kDa). The distances of dye migration ranged from 200 to 250 μm. The dye transfer extent of the cells with HMW HA added was lower than that of the control, indicating that GJIC decreased in the HMW HA- [310 kDa (data not shown) and 800 kDa] added cells [Fig. 3 (see I and II) and Fig. 4].

In contrast, strongly enhanced dye transfer is observed in the cells cultured on dish surfaces coated with various HA [Fig. 3 (see III) and Fig. 4]. Furthermore, there was no difference in cell viability between the coating and the addition methods (Fig. 5). It would seem that the increase of dye transfer is influenced by ionic interaction between HMW HA molecules and nutrients in medium, as shown in Figure 6. As a result, the NHDF cells can use these nutrients and the nutrient-enriched substrate like natural extracellular matrix by the binding of HMW HA to various kinds of cytokines, such as bFGF, TGF-β, etc. This might play an important role in the increase of GJIC.

Enhancement of GJIC by bFGF and TGF-β has been reported,[16,17] and the function of GJIC was considered to be a useful marker for evaluating tissue-engineered products.[18] In the case of LMW HA, GJIC function was higher in the coated than it was with the added LMW HA although there was no statistically significant difference between the two groups (Fig. 4 and Fig. 6).

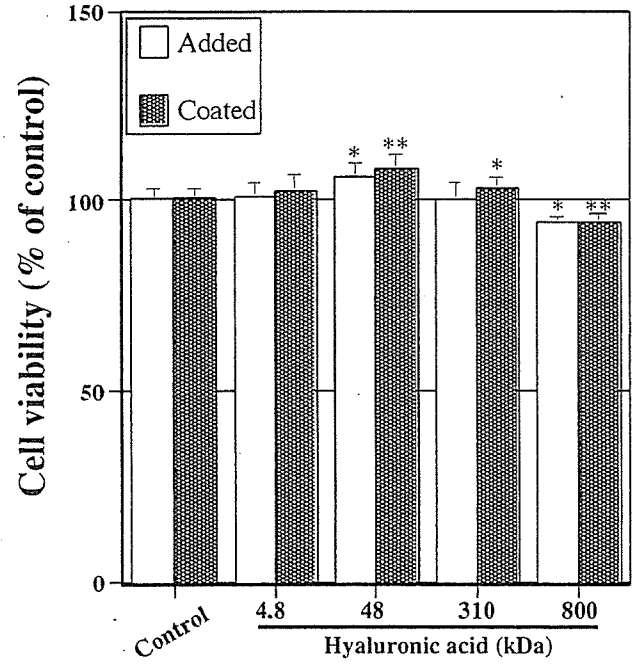

Figure 5. Cell viability of NHDF cells cultured with various HA estimated by alamarBlue™ assay.

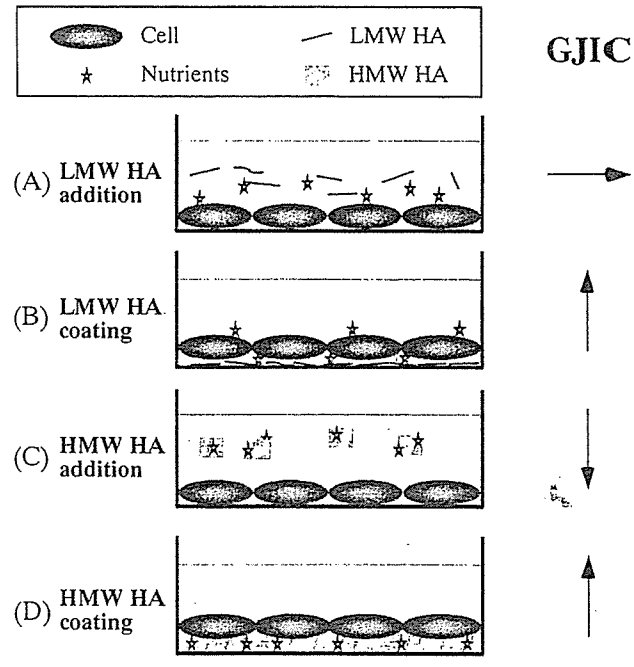

Figure 6. Basic concept of the different extent of the GJIC function under four kinds of culture conditions of NHDF cells: (A) no effect on the function of GJIC by the addition of LMW HA; (B) enhancement of the function of GJIC by the coating of LMW HA; (C) inhibition of the function of GJIC by the addition of HMW HA; and (D) enhancement of the function of GJIC by the coating of HMW HA.